P. Lopez-Crespo et alii, Frattura ed Integrità Strutturale, 41 (2017) 203-210; DOI: 10.3221/IGF-ESIS.41.28

Focused on Crack Tip Fields

Mid-thickness studies of the stress intensity factor in the bulk of bainitic steel

P. Lopez-Crespo, J. Vazquez-Peralta
Department of Civil and Materials Engineering, University of Malaga, C/Dr Ortiz Ramos s/n, 29071 Malaga, Spain
plopezcrespo@uma.es

C. Simpson
School of Materials, University of Manchester, Oxford Road, Manchester M13 9PL, UK

T. Buslaps
European Synchrotron Radiation Facility (ESRF), 6 rue J Horowitz, 38000 Grenoble, France

P. J. Withers
School of Materials, University of Manchester, Oxford Road, Manchester M13 9PL, UK
Research Complex at Harwell, Didcot, Oxfordshire, OX11 0FA, UK.

ABSTRACT. The current work aims at estimating the stress intensity factor deep inside the bulk from elastic strain data measured by synchrotron X-ray diffraction. Key features affecting the evaluation of the stress intensity factor are the number of terms in the analytical model describing the crack tip field, the extension and position of the area of interest of the experimental data, the effect of the experimental data collected within the plastic zone and the number of elastic strain data points used. Here a parametric study of these features is presented in terms of their influence for the stress intensity factor determination. It was found that 3 or 4 terms in Williams' expansion is often sufficient; the data should be collected from across the full range of angles around the crack tip; and the number of points/number of terms should be greater than 40.

KEYWORDS. Stress intensity factor; Bainitic steel; Williams' expansion; X-ray diffraction.

Citation: P. Lopez-Crespo, J. Vazquez-Peralta, C. Simpson, T. Buslaps, P. J. Withers, Mid-thickness studies of the stress intensity factor in the bulk of bainitic steel , Frattura ed Integrità Strutturale, 41 (2017) 203-210.

Received: 28.02.2017
Accepted: 15.04.2017
Published: 01.07.2017

INTRODUCTION

The experimental characterisation of crack tip fields is normally done using surface techniques such as photo-elasticity [1], Moiré interferometry [2], thermo-elastic stress analysis [3], electronic speckle pattern interferometry [4] or digital image correlation [5,6]. For thin components, the surface behaviour is normally representative of the

complete behaviour [7]. However, for many engineering components, the surface may not be at all representative of the majority of the bulk of the material [8,9] and not describe accurately the complete component behaviour [10,11]. Intense hard X-ray beams at synchrotron facilities now give us the possibility of probing the bulk of engineering materials both in terms of the geometry and in terms of elastic strain. Geometrical features of the crack can be studied through synchrotron X-ray micro-tomography [12,13]. Elastic strains can be investigated through synchrotron X-ray diffraction [14,15]. Synchrotron X-ray diffraction can also be used to obtain the J-integral [16]. In this work synchrotron X-ray diffraction is used to estimate the SIF deep within the bulk of a cracked specimen. The methodology combines a mathematical model describing the elastic crack tip field and elastic strain data obtained experimentally by synchrotron X-ray diffraction. First, the material and specimen employed are described. Then, details about the experimental setup for strain measurement are given. This is followed by an explanation of how experimental data and the analytical model are combined to extract the SIF. Finally, the influence of key parameters affecting the estimation of the SIF is studied.

MATERIALS AND METHODS

The tests were undertaken on a bainitic steel similar to Q1N having the chemical composition shown in Tab. 1. The material exhibited a Yield Stress σ_y=690 MPa, Ultimate Tensile Stress σ_{uts}=858 MPa and very fine grain that allowed high quality high spatial resolution strain data to be collected [17]. The bainitic steel also has a good combination of fatigue resistance and low environmental impact for applications where no energy is consumed during the use phase of the component [18]. The fatigue tests were conducted on a Compact Tension (CT) specimen of 60 mm width and 3.3 mm thickness (Fig. 1).

Alloy	C	Si	Mn	P	S	Cr	Ni	Mo	Cu
Q1N	0.16	0.25	0.31	0.010	0.008	1.42	2.71	0.41	0.10

Table 1: Chemical composition in weight % of Q1N steel. The balance is Fe.

3000 cycles were applied in the pre-cracking stage of the experiment at a frequency of 10 Hz. During the pre-cracking stage, the stress intensity range, ΔK, was approximately 35 MPa√m and the load ratio, P_{min}/P_{max}, 0.03. Plane stress conditions dominated through the thickness for all loads applied during the experiment, since each XRD measurement included information over 1.4 mm through the thickness [19]. The crack length was measured perpendicular to the loading direction from the centre of the loading holes [20].

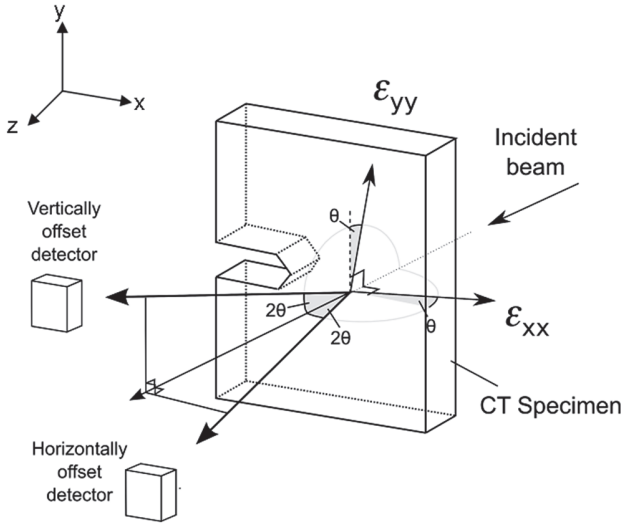

Figure 1: Illustration of beam and Compact Tension specimen configuration.

MAPPING OF ELASTIC STRAIN

The strain mapping experiments were conducted on beamline ID15A of the European Synchrotron Radiation Facility (France). Energy dispersive mode was used, following the configuration previously applied with high qauality results [15,21]. Two solid state X-ray detectors were mounted to measure two in-plane directions of strain (ε_{xx} and ε_{yy}). The scattering angle was $2\theta = 5^{o}$. The elastic strain was evaluated according to Bragg's law:

$$\varepsilon_{hkl} = \frac{d_{hkl} - d^{0}_{hkl}}{d^{0}_{hkl}} \tag{1}$$

where d_{hkl} is the lattice parameter of crystallographic plane (hkl) measured at a certain load and d^{0}_{hkl} is the strain-free lattice parameter of the same crystallographic plane. Here the plane (211) was used. The incident beam slits were opened to 60 × 60 μm, giving a lateral resolution (x, y) of 60 μm and a nominal gauge length through-thickness (z) of around 1.4 mm [17]. The gauge length was diamond shaped and centred on the mid-plane (z=0). Attention was paid to locate the origin of coordinates at the crack tip [22]. Fig. 2 shows an elastic strain field in the crack opening direction for a sample subjected to 5.3 kN. The two black solid lines in Fig. 2 emanating from the origin of coordinates towards negative coordinates in the crack growing direction represent the crack.

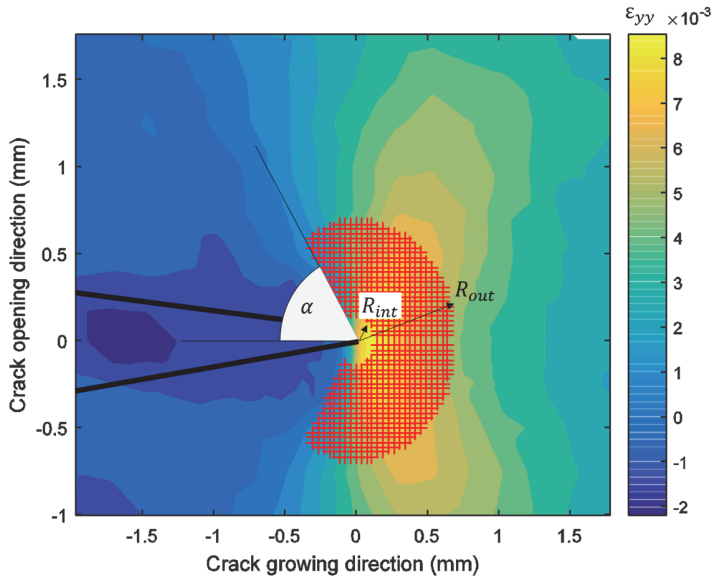

Figure 2: The elastic strain field based on the (211) peak local to the crack in the crack opening direction (ε_{yy}) for a 13 mm crack length subjected to 5.3 kN. The area sampled by each point is 60 x 60 μm. The parameters relating to the area of interest are also illustrated: inner radius of the data array, R_{int}, outer radius of the data array, R_{out}, and angle between the end of the data array and the crack plane, α.

FITTING THE EXPERIMENTAL TO AN ELASTIC MODEL

The elastic strains were fitted to an analytical model following a multi-point over-deterministic scheme [23]. The analytical model was based on Williams' series development used to describe the elastic behaviour of the region surrounding the crack tip [24]. The strains in the crack opening direction can be written as [25]:

$$E\varepsilon_{yy} = A_0 r^{-\frac{1}{2}} \cos\frac{\theta}{2}\left[(1-\upsilon)+(1+\upsilon)sin\frac{\theta}{2}sin\frac{3\theta}{2}\right] - 2\upsilon B_0 + A_1 r^{\frac{1}{2}} \cos\frac{\theta}{2}\left[(1-\upsilon)-(1+\upsilon)sin^2\frac{\theta}{2}\right]$$

$$-2\upsilon B_1 r\cos\theta+\frac{A_2}{2}r^{\frac{3}{2}}\left[2(1-\upsilon)\cos\frac{3\theta}{2}+3(1+\upsilon)\sin\theta\sin\frac{\theta}{2}\right]+2B_2r^2\left[-\upsilon+(3\upsilon+1)\sin^2\theta\right] \quad (2)$$

where E is the Young's modulus, ε_{yy} are the strains in the crack opening (vertical) direction, A_n and B_m are unknown coefficients or number of terms in the series expansion, r and θ are the polar coordinates of the different points around the crack tip and υ is the Poisson's ratio. The singular term, A_0 can be related to the SIF as:

$$A_0=\frac{K_I}{\sqrt{2\pi}} \quad (3)$$

Substitution of all experimental data points in Eq. (2) yields an over-deterministic system of equations that can be solved for the unknown coefficients and thereby computing the SIF (K_{exp}).

PARAMETRIC STUDY

The evaluation of the key parameters involved in the estimation of the SIF, K_{exp}, is done through comparison with the theoretical SIF, K_{theo} [20]. To this end, the error between both values can be determined as:

$$error(\%)=\left|\frac{K_{exp}-K_{theo}}{K_{theo}}\right|\times 100 \quad (4)$$

Key parameters influencing the K estimation with the current scheme were identified previously [26,27]. These include the number of terms used in Williams' expansion, the size and shape of the area of interest (AOI) used for the fitting, the influence of the plastic zone and the number of experimental data points considered.

Number of terms, size and shape of the area of interest

The size of the AOI is studied through the outer radius of the AOI, R_{out}, defined in Fig. 2. The combined influence of number of terms and size of AOI is shown in Fig. 3.

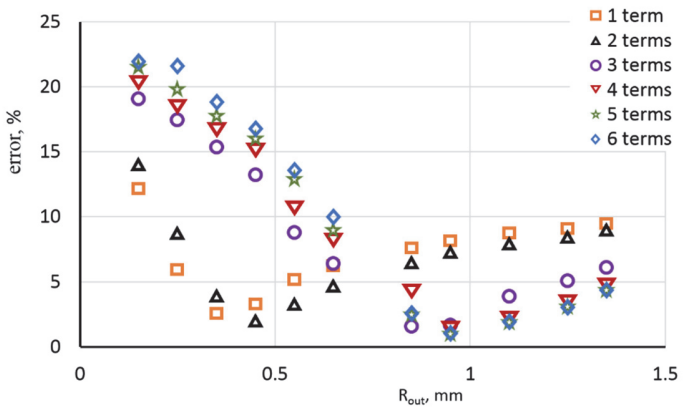

Figure 3: Effect of number of terms and size of the AOI (R_{out}) on the error in estimating the SIF.

Fig. 3 shows that the error decreases to a minimum for each value of number of terms studied. The minimum error as a function of R_{out} observed is summarised in Tab. 2.

Number of terms	1	2	3	4	5	6
R_{out} (μm)	350	450	850	950	950	950

Table 2: Combination of number of terms and outer radius, R_{out}, that give a minimum error in Fig. 3

Tab. 2 can be used as a reference to optimise the data array to be used depending on how many terms in Williams' expansion are chosen to describe the crack-tip field. Tab. 2 indicates that if one term is used in Williams' formultion, the data array should extend to around 350 μm and for six terms the array should extend to around 950 μm. Fig. 3 also shows that by using more terms in the series expansion, the error in estimating the SIF can be reduced to around 1%.

The shape of the AOI was studied through the angle between the edge of the AOI and the crack plane, α (see Fig. 2). The angle α controls the number of data points that are collected from the region behind the crack tip (negative coordinates along the crack growing direction, Fig. 2). The amount of data collected in the crack wake has been previously identified as critically affecting the SIF estimation [27]. Fig. 4 shows the evolution of the error for different α angles. For each number of terms, the optimum outer radius was used, following the results of Tab. 2.

When only 1 term is used the curve in Fig. 4 is very flat such that in our case a slightly better result is obtained for α=80 than 0°. In view of this, the conclusion would be that results become more reliable for >2 terms and that the best SIF predictions (minimum error) are obtained when α = 0º when using 3 to 6 terms in Williams' expansion. That is, the best results in terms of estimating the SIF are obtained by collecting data not only ahead of the crack tip but also from the crack wake region, in agreement with previous studies [27].

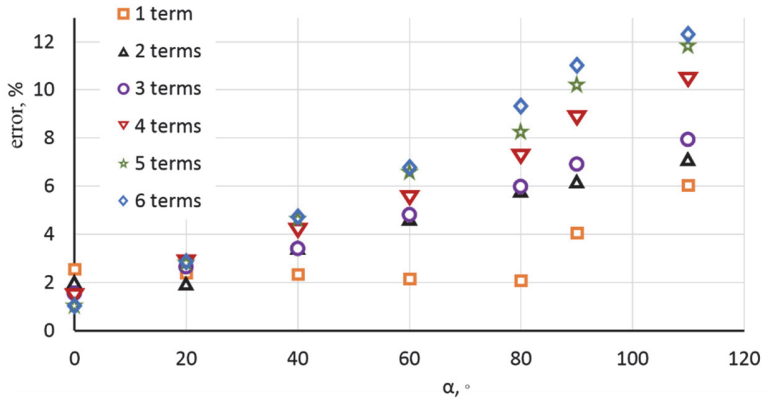

Figure 4: Effect of α angle on the error for estimating the SIF.

Plastic zone

The mathematical model used to describe the crack-tip behaviour is based on Linear Elastic Fracture Mechanics. Accordingly, the tool can be used under small scale yielding (SSY) conditions. For other full-field techniques such as thermo-elasticity [3], photo-elasticity [1], digital image correlation [28] or electronic speckle patter interferometry [4], this is achieved by collecting data from outside the plastic zone. This effect is studied here by including and excluding the data from the plastic zone in the data used for estimating the SIF. The plastic zone was estimated according to Irwin model [25]:

$$r_{pz} = \frac{1}{2\pi}\left(\frac{K}{\sigma_y}\right)^2 = 330\mu m \tag{5}$$

where K is the theoretically applied SIF and σ_y is the yield stress of the material. Fig. 5 shows the error obtained when the plastic zone is included or excluded. The best predictions are observed when the plastic zone data is used in the fitting. Fig. 5 also shows that there are large differences between including and excluding the plastic zone for 1 term. This difference decreases as the number of terms is increased. The worst prediction when the plastic zone is excluded is probably due to not having enough data for the over-deterministic system of equations. This effect is studied in more detail in the following section.

Number of experimental data points

The effect the number of experimental data points that are fitted into the analytical model is studied in this section. The number of data points is studied relative to the number of terms in the series (Eq. 2) through parameter φ:

$$\varphi = \frac{number\ of\ data\ points}{number\ of\ terms\ in\ series} \tag{6}$$

Fig. 6 shows the error for different levels of φ parameter. φ parameter represents the level of over-determination in the system of equations. Fig. 6 shows that increasing φ parameter produces better estimations of the SIF. The best estimations are observed for higher terms (5 and 6). For φ ≥40, the error is below 5%. For φ = 20 the error is smaller than 10% for all number of terms studied.

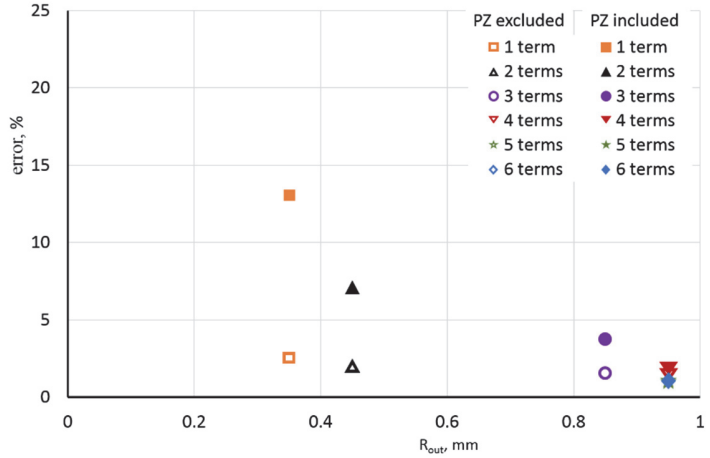

Figure 5: Effect of including or excluding the plastic zone in the collected data, i.e. setting R_{int}=0 or setting R_{int}=330μm.

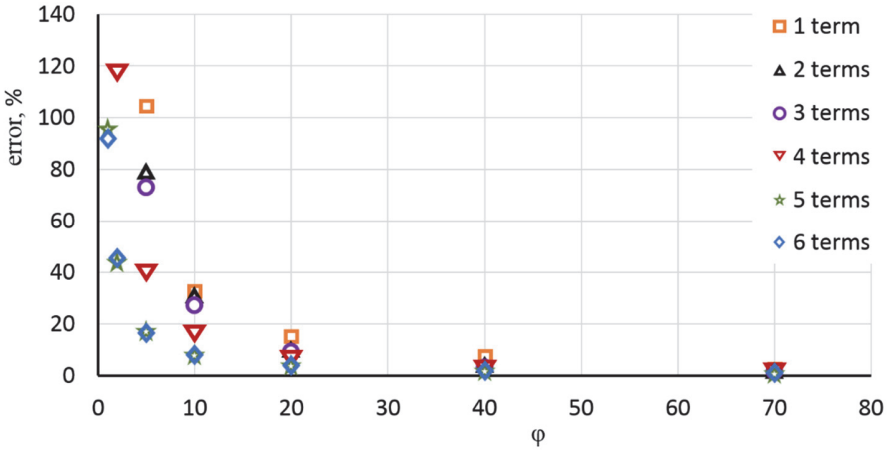

Figure 6: Effect of the level of over-determination (i.e. φ parameter, as defined in Eq. 6).

Conclusions

A novel approach for estimating the SIF inside the bulk of engineering materials is described. The approach is based on fitting experimental data on an analytical model following a multi-point over-deterministic scheme. The experimental data are collected from the bulk of the material through powerful synchrotron X-ray diffraction. The analytical model describing the elastic field around the crack-tip is based on Williams development. The methodology is applied to a CT specimen made of bainitic steel. A detailed analysis of key parameters affecting the efficacy of the SIF evaluation is presented. The current study suggests that:

1. 3 or 4 terms in Williams's expansion is often sufficient.
2. Data points should be included from across the full range of angles in front and behind the crack tip.

3. A outer radius of at least the size of the plastic zone was needed.
4. Little advantage was obtained by excluding the plastic zone.
5. To get accurate results the number of data points/number of terms should be $\varphi \geq 40$.

Of course in our case the plastic zone is not especially well developed (i.e. it is still well within the LEFM regime) different conclusions may apply in the case of extensive plastic deformation local to the crack.

ACKNOWLEDGEMENTS

The authors would like to acknowledge financial support of Junta de Andalucía through Proyectos de Excelencia grant reference TEP-3244, Campus de Excelencia Internacional del Mar (CEIMAR) and Ministerio de Economía y Competitividad through grant reference MAT2016-76951-C2-2-P. PJW acknowledges European Research Council Funding (CORREL-CT grant number 695638 and EPSRC Funding under the following grants EP/M010619, EP/K004530, EP/F007906, EP/F028431 and EP/I02249X/1. The authors are also grateful to the ESRF for ID15 beamtime awarded under MA-1483.

REFERENCES

[1] Nurse, A.D., Patterson, E.A., Determination of predominantly mode II stress intensity factors from isochromatic data. Fatigue and Fracture of Engineering Materials and Structures, 16 (1993) 1339–1354.
[2] Nicoletto, G., Experimental crack tip displacement analysis under smallscale yielding conditions. International Journal of Fatigue, 8 (1986) 83–89.
[3] Diaz, F.A., Yates, J.R., Patterson, E.A., Some improvements in the analysis of fatigue cracks using thermoelasticity. International Journal of Fatigue, 26 (2004) 365–376.
[4] Shterenlikht, A., Díaz-Garrido, F.A., Lopez-Crespo, P., Withers, P.J., Patterson, E.A., Mixed Mode (KI + KII) Stress Intensity Factor Measurement by Electronic Speckle Pattern Interferometry and Image Correlation, Applied Mechanics and Materials, 1-2 (2004) 107–112.
[5] Yoneyama, S., Morimoto, Y., Takashi, M., Automatic evaluation of mixed-mode stress intensity factors utilizing digital image correlation, Strain, 42 (2006) 21–29.
[6] Lopez-Crespo, P., Shterenlikht, A., Patterson, E.A., Withers, P.J., Yates, J.R., The stress intensity of mixed mode cracks determined by digital image correlation, Journal of Strain Analysis for Engineering Design, 43 (2008) 769–780. DOI: 10.1243/03093247JSA419.
[7] Lopez-Crespo, P., Withers, P.J., Yusof, F., Dai, H., Steuwer, A., Kelleher, J.F., Overload effects on fatigue crack-tip fields under plane stress conditions: surface and bulk analysis, Fatigue and Fracture of Engineering Materials and Structures, 36 (2013) 75–84.
[8] de-Matos, P.F.P., Nowell, D., Experimental and numerical investigation of thickness effects in plasticity-induced fatigue crack closure, International Journal of Fatigue, 31 (2009) 1795–1804.
[9] Yusof, F., Lopez-Crespo, P., Withers, P.J., Effect of overload on crack closure in thick and thin specimens via digital image correlation, International Journal of Fatigue, 56 (2013) 17–24.
[10] Garcia-Manrique, J., Camas, D., Lopez-Crespo, P., Gonzalez-Herrera, A., Stress intensity factor analysis of through thickness effects, International Journal of Fatigue, 46 (2013) 58–66.
[11] Camas, D., Lopez-Crespo, P., Gonzalez-Herrera, A., Moreno, B., Numerical and experimental study of the plastic zone in cracked specimens, Engineering Fracture Mechanics, (2017). DOI:10.1016/j.engfracmech.2017.02.016.
[12] Withers, P.J., Lopez-Crespo, P., Kyrieleis, A., Hung, Y.-C., Evolution of crack-bridging and crack-tip driving force during the growth of a fatigue crack in a Ti/SiC composite, Proceedings of the Royal Society A Mathematical, Physical and Engineering Sciences, 468 (2012) 2722–1743.
[13] Maire, E, Withers, P.J., Quantitative X-ray tomography. International Materials Reviews, 59 (2014) 1–43. DOI: 10.1179/1743280413Y.0000000023.
[14] Withers, P.J., Use of Synchrotron X-ray Radiation for Stress Measurement. In: M E Fitzpatrick AL, editor. Analysis of Residual Stress by Diffraction using Neutron and Synchrotron Radiation, London: Taylor & Francis; (2003) 170–189.
[15] Lopez-Crespo, P., Mostafavi, M., Steuwer, A., Kelleher, J.F., Buslaps, T., Withers, P.J., Characterisation of overloads in fatigue by 2D strain mapping at the surface and in the bulk, Fatigue & Fracture of Engineering Materials & Structures, 39 (2016) 1040–1048.

[16] Barhli, S.M., Saucedo-Mora, L., Simpson, C., Becker, T., Mostafavi, M., Withers, P.J., Obtaining the J-integral by diffraction-based crack-field strain mapping, Procedia Structural Integrity, 2 (2016) 2519–2526.
[17] Lopez-Crespo, P., Steuwer, A., Buslaps, T., Tai, Y.H., Lopez-Moreno, A., Yates, J.R., Measuring overload effects during fatigue crack growth in bainitic steel by synchrotron X-ray diffraction, International Journal of Fatigue, 71 (2015) 11–16.
[18] Chaves, V., Ecological criteria for the selection of materials in fatigue. Fatigue & Fracture of Engineering Materials & Structures, 37 (2014) 1034–1042. DOI: 10.1111/ffe.12181.
[19] Anderson, T.L., Fracture mechanics: fundamentals and applications, 2nd ed. Boca Raton: CRC Press; (1994).
[20] Murakami, Y., Stress Intensity Factors Handbook. Oxford: Pergamon Press; (1987).
[21] Steuwer, A., Rahman, M., Shterenlikht, A., Fitzpatrick, M.E., Edwards, L., Withers, P.J., The evolution of crack-tip stresses during a fatigue overload event, Acta Materialia, 58 (2010) 4039–4052.
[22] Zanganeh, M., Lopez-Crespo, P., Tai, Y.H., Yates, J.R., Locating the crack tip using displacement field data: a comparative study, Strain, 49 (2013) 102–115.
[23] Sanford, R.J., Dally, J.W., A general method for determining mixed-mode stress intensity factors from isochromatic fringe patterns, Engineering Fracture Mechanics, 11 (1979) 621–633.
[24] Williams, M.L., On the stress distribution at the base of a stationary crack. Journal of Applied Mechanics, 24 (1957) 109–114.
[25] Ewalds, H.L., Wanhill, R.J.H., Fracture Mechanics. London: Arnold; (1984).
[26] Lopez-Crespo, P., Moreno, B., Lopez-Moreno, A., Zapatero, J., Characterisation of crack-tip fields in biaxial fatigue based on high-magnification image correlation and electro-spray technique, International Journal of Fatigue, 71 (2015) 17–25.
[27] Mokhtarishirazabad, M., Lopez-Crespo, P., Moreno, B., Lopez-Moreno, A., Zanganeh, M., Evaluation of crack-tip fields from DIC data: a parametric study, International Journal of Fatigue, 89 (2016) 11–19.
[28] Yoneyama, S., Ogawa, T., Kobayashi, Y., Evaluating mixed-mode stress intensity factors from full-field displacement fields obtained by optical methods, Engineering Fracture Mechanics, 74 (2007) 1399–1412.